Ann. Geophys. Discuss.,
https://doi.org/10.5194/angeo-2018-63-AC1, 2018

Annales Geophysicae Discussions

Interactive comment on "Local time extent of magnetopause reconnection X-lines using space–ground coordination" *by* Ying Zou et al.

Ying Zou et al.

yingzou@bu.edu

Received and published: 27 September 2018

Reviewer comment: The authors discuss conjugate observations of two THEMIS satellites crossing the magnetopause in short succession, with ground based radar observations to determine the lengths of a dayside reconnection line at the magnetopause. The methodology seems to be interesting and the paper is well written with a very good introduction to the general problem. However I have some issues with the current data analysis and the event selection that are significant enough to not recommend publication at this time. General Point: As the authors admit, their determined length of the X-line will be limited to the longitudinal coverage of the radars. This unavoidable limitation will always significantly influence their conclusion about the length of the "actual" X-line, which could be considerably longer, and will prevent them from ever finding

a global answer. That will seriously limit the usefulness of the methodology, thought generally its an interesting approach.

Response: We realize that the term "X-line extent" in our manuscript has caused confusion. The X-line the reviewer refers to is the magnetic geometry along which reconnection occurs at various rates and frequencies, which is indeed considerably longer than the radar coverage. However, our study intends to focus on the extent of reconnection bursts. We have revised the term "X-line extent" to "reconnection burst extent" as we do not aim at determining the extent of the global X-line but the localized bursty reconnection in the area of satellite-ground conjunction. Other bursts could occur outside the radar and satellite coverage but those are beyond the focus of this research. Please see also the response to the next comment. With this clarification, the radar longitudinal coverage is sufficiently large for the purpose of this study. For example, the ionospheric flow structures under examination have a skewed Gaussian-shape velocity profile (Figures 2e, 4e, and 6e), and the FWHM of the profile is located completely within the radar coverage.

Reviewer comment: About the introduction: There are several significant publications using IMAGE/FUV observations. This mission had the ability to observe emissions from precipitating (cusp) ions over the entire polar region at once and was therefore not limited like the radar coverage in the present manuscript. Studies using these data have shown evidence that during southward IMF conditions the entire dayside is open leading to very long dayside reconnection lines. So, based on these results the length of the X-line is not the driving question. In additions, decades of cusp observations in all local time sectors show precipitating ions. X-lines in general seem to be very long. Cusp observations have shown that a substantial part of reconnection is dominated by pulsed reconnection [Lockwood et al.,. . ...]. The question is therefore – is the long X-line pulsing as "One" or are individual longitudinal sections have their own pulsation frequency? That should lead to scenarios presented in this manuscript, sections of X-lines that are active next to sections of X-lines temporarily inactive. This is how I

would interpret the observations in the manuscript. Therefore the conclusion would not be about the length of the X-line since that would be masked by the temporal nature of the reconnection process, which might lead to misleading results. In any case, I was surprised that there was no reference to this rather ground breaking IMAGE observations anywhere. These observations [e.g., Fuselier et al., 2002] should be added in the introduction and properly described.

Response: As the reviewer inferred we examine bursts of reconnection. Our study shows that a reconnection burst is not necessarily a pulse of a long X-line but can occur over a finite area. IMAGE observations have provided global configuration of reconnection where reconnection bursts are embedded. The global-scale reconnection configuration is not the focus of this study but it offers valuable groundwork of clarifying the scope of the research. We rewrite the first paragraph as "...Reconnection tends to occur at sites of strictly anti-parallel magnetic fields as anti-parallel reconnection [e.g. Crooker, 1979; Luhmann et al., 1984], or occur along a line passing through the subsolar region as component reconnection [e.g. Sonnerup, 1974; Gonzalez and Mozer, 1974]. Evidence shows either or both can occur at the magnetopause and the overall reconnection extent can span from a few to 40 Re [Paschmann et al., 1986; Gosling et al., 1990; Phan and Paschmann, 1996; Coleman et al., 2001; Phan et al., 2001, 2003; Chisham et al., 2002, 2004, 2008; Petrinec and Fuselier, 2003; Fuselier et al., 2002, 2003, 2005, 2010; Petrinec and Fuselier, 2003; Pinnock et al., 2003; Bobra et al., 2004; Trattner et al., 2004, 2007, 2008, 2017; Trenchi et al., 2008]. However, reconnection does not occur uniformly across this configuration but has spatial variations [Pinnock et al., 2003; Chisham et al., 2008]. The local time extent of reconnection bursts is the focus of this study."

Reviewer comment: Specific Points: Line 188: the D-shaped distribution do not persist into the ionosphere due to the conservation of the first adiabatic invariant. The D shape changes into a Crescent shape as soon as the ambient B field increases, which it definitely will in the cusps. This has been observed in the cusp regions for decades.

This effect is so pronounced that it can be even used directly at the magnetopause. The "bending over" of the D-shape distribution observed during magnetopause crossings has been used in a recent study by Broll et al. (2017) (JGR) to determine the distance to the X-line from the MMS satellites and infer the X-line location. Cusp Steps have nothing to do with D-shape distributions. Cusp steps are the result of changes in the reconnection rate at the magnetopause or caused by spatially separated X-lines. Cusp-steps have been discussed in great detail by Lockwood and Smith in the 90ties as manifestation of pulsed reconnection leading to the pulsed reconnection model and by e.g., Onsager et al [1995] or Trattner et al. [2002] as spatially separated X-lines.

Response: We agree with the reviewer and correct the statement as "The D-shaped ion distributions are deformed into a crescent shape as ions travel away from the reconnection site [Broll et al., 2017]". We also replace case study #1 with a new event and the new event has a distorted D-shaped distribution. Details can be found below.

Reviewer comment: The authors use patchy reconnection also in the case of spatially separated X-line or partial X-lines. This will be a source of confusion for colleagues not too familiar with the subject. Patchy reconnection usually describes pulsed reconnection – temporal changes in reconnection. While the authors do a reasonable good job in trying to keep the temporal and spatial regimes apart I would recommend to revisit that issue throughout the paper.

Response: We follow the reviewer's suggestion and add "the term patchy has also been used to describe the temporal characteristics of reconnection [e.g. Newell and Meng, 1991]. But this paper primarily focuses on the spatial properties". We use "spatially patchy reconnection" to replace "patchy reconnection" throughout the text.

Reviewer comment: Figure 2: The symbol for Th-D is completely invisible – if it wasn't for Figure 4 I would not have realized that there are indeed two separate magnetic foot points in that plot. Chose a different more prominent color.

Response: As advised by the reviewer we replace this event with an event that has

good field line mapping. Please find the attachment for the new event.

Reviewer comment: Figure 2: it is mentioned in line 209 – the satellite foot points should map close to the radars FOV. I would recommend that the authors look for events where the satellite foot points are actually in the FOV of the radars to make absolutely sure that these observations are linked. Throughout the paper but especially in Figure 2 I do not have the impression that this is the case which makes the data analysis rather questionable. Therefore I fail to see how the observed D-shape distributions at the magnetopause are connected with particular flow channels which is the essential part of the study. The authors also mark the cusp foot point in the radar images. Discussing again the events in figure 2, Th-D clearly saw an ion jet. It therefore observed reconnection at the magnetopause and was on a newly opened field line. The D shape distribution, while looking a bid crooked compared to the other D-shape distributions in the manuscript, travels along the magnetic field. The magnetic field, at that time the distribution was observed, was still northward. Therefore the satellite was in the LLBL and the ions move toward the northern cusp where the radar observations observe flow channels. All open magnetopause field lines map into the cusps. So the Th-D magnetic foot point, were the D-distribution was observed, should be in that region marked as cusp in figure 2d. It is not, its not even in the FOV for the radar.

Response: To address reviewer's comment, we replace Figures 1-2 (see Figures 1-2). In the new event the footprint is within the radar FOV and close to the open-closed field line boundary. The corresponding text is changed to the following.

"3.1.1 In-situ satellite measurements

On February 2, 2013, THA and THE made simultaneous measurements of the dayside magnetopause with a 1.9 Re separation in the Y direction around 21:25 UT. The IMF condition is displayed in Figure 1a and the IMF was directed southward. The satellite location in the GSM coordinates is displayed in Figure 1b, and the measurements are presented in Figure 2. The magnetic field and the ion velocity components are

displayed in the LMN boundary normal coordinate system, where L is along the outflow direction, M is along the X-line, and N is the current sheet normal. The coordinate system is obtained from the minimum variance analysis of the magnetic field at each magnetopause crossing [Sonnerup and Cahill, 1967]. Figures 2g-p show that both satellites passed from the magnetosheath into the magnetosphere, as seen as the sharp changes in the magnetic field, the ion spectra, and the density (shaded in pink).

As THE crossed the magnetopause boundary layer (2122:57-2123:48 UT), it detected both fluid and kinetic signatures of reconnection. It observed a rapid, northward-directed plasma jet within the region where the magnetic field rotated (Figures 2g and 2j). The magnitude of this jet relative to the sheath background flow reached 262 km/s at its peak, which was 72% of the predicted speed of a reconnection jet by the Walen relation (366 km/s, not shown). The angle between the observed and predicted jets was 39°. The ion distributions in Figure 2k showed a distorted D-shaped distribution similar to the finding of by Broll et al. [2018]. The distortion is due to particles traveling in the field-aligned direction from the reconnection site to higher magnetic field region, and Broll et al. [2018] estimated the traveling distance to be a few Re for the observed level of distortion.

THA crossed the magnetopause one to two minutes later than THD (2124:48-2125:13 UT). While it still identified a plasma jet at the magnetopause (Figures 2l and 2o), the jet speed was significantly smaller than what was predicted for a reconnection jet (80 km/s versus 380 km/s in the L direction). The observed jet was directed 71° away from the prediction. The ion distributions deviated from clear D-shaped distributions (Figure 2p). Reconnection was thus much less active at THA local time than at THE. This suggests that the X-line of the active reconnection at THE likely did not extend to THA.

3.1.2 Ground radar measurements

The velocity field of the dayside cusp ionosphere during the satellite measurements is shown in Figures 2a-c. Figure 2a shows the radar LOS measurements at 21:25 UT,

as denoted by the color tiles, and the merged vectors, as denoted by the arrows. The colors of the arrows indicate the merged velocity magnitudes, and the colors of the tiles indicate the LOS speeds that direct anti-sunward (those project to the sunward direction appear as black). Fast (red) and anti-sunward flows are the feature of our interest. One such of this flow can be identified in the pre-noon sector, which had a speed of $\sim$800 m/s and was directed poleward and westward. As the merged vector arrows indicate, the velocity vectors have a major component close to the INV beam directions and thus the INV LOS velocities reflect the flow distribution. The flow crossed the open-closed field line boundary, which was located at 78° MLAT based on the spectral width (Figure 2d and S1). This flow thus meets the criteria of being an ionospheric signature of magnetopause reconnection. Another channel of fast flow was present in the post-noon sector. This post-noon flow was directed more azimuthally and was separated from the pre-noon flow by a region of slow velocities at >79° MLAT around noon. The two flows are thus two different structures likely originating from two discontinuous reconnection bursts. Since the satellites were located in the pre-noon sector we focus on the pre-noon flow below.

The flow had a limited azimuthal extent. The extent is determined at half of the maximum flow speed, which was $\sim$400 m/s. Figure 2f discussed below shows a more quantitative estimate of the extent. In Figure 2a, we mark the eastern and western boundaries with the dashed magenta lines, across which the LOS velocities dropped from red to blue/green colors.

Figure 2b shows the SECS velocities, denoted by the arrows. The SECS velocities reasonably reproduced the spatial structure of the flows seen in Figure 2a. The flow boundaries were marked by the dashed magenta lines, across which the flow speed dropped from red to blue. Across the flow western boundary the flow direction also reversed. The equatorward-directed flows are interpreted as the return flow of the poleward flows, as sketched in Southwood [1987] and Oksavik et al. [2004].

The velocity field reconstructed using the SHF velocities is

shown in Figure 2c (obtained through the Radar Software Toolkit (http://superdarn.thayer.dartmouth.edu/software.html)). This is an expanded view of the global convection maps in Figure S2 focusing on the dayside cusp and the employed radars listed in Section 2 have contributed to the majority of the backscatters on the dayside. The SHF velocities also captured the occurrence of two flows in the pre- and post-noon sectors, respectively, although the orientation of the flows were less azimuthally-aligned than Figure 2a or 2b. The difference is likely due to the contribution from the statistical potential distribution under the southward IMF. The flow western and eastern boundaries were again marked by the dashed magenta lines.

Figure 2d shows spectral width measurements. Large spectral widths can be produced by soft ($\sim$100 eV) electron precipitation [Ponomarenko et al., 2007] such as cusp/mantle precipitation, and evidence has shown that the longitudinal extent of large spectral widths correlates with the extent of PMAFs [Moen et al., 2000] and of poleward flows across the OCB [Pinnock and Rodger, 2001]. Large spectral widths thus have the potential to reveal the reconnection burst extent. For the specific event under examination, the region of large spectral widths, appearing as red color, spanned from 10.5 to 14.5 h MLT if we count the sporadic scatters in the post-noon sector. This does not contradict the flow width identified above because the wide width reflects the summed width of the pre- and post-noon flows. In fact a more careful examination shows the presence of two dark red (>220 m/s spectral width) regions embedded within the $\sim$200-m/s spectral widths (circled in red, the red dashed line is due to the discontinuous backscatters outside the INV FOV), corresponding to the two flows.

Figures 2a-c all observed a channel of fast anti-sunward flow in the pre-noon sector of the high latitude ionosphere, and the flow had a limited azimuthal extent. If the flow corresponded to magnetopause reconnection, the X-line is expected to span over a limited local time range. This is consistent with the THEMIS satellite observation in Section 3.1.1, where THE at Y = -2.9 Re detected clear reconnection signatures, while THA at Y = -4.8 Re did not. In fact, if we project the satellite location to the

ionosphere through field line tracing under the T89 model, THE was positioned at the flow longitude, while THA outside the flow was to the west (Figure 2a).

While this paper primarily focuses on the spatial extent of reconnection bursts, the temporal evolution of reconnection can be obtained from the time series plot in Figure 2e. Figure 2e presents the INV LOS measurements along 80° MLAT (just poleward of the open-closed field line boundary with good LOS measurements) as functions of magnetic longitude (MLON) and time. Similar to the snapshots, the color represents LOS speeds that project to the anti-sunward direction, and the flow of our interest appears as a region of red color. The time and the location where THA and THE crossed the magnetopause are marked by the vertical and horizontal lines. The flow emerged from a weak background at 2120 UT and persisted for $\sim$30 min in INV FOV. At the onset the flow eastern boundary was located at -82° MLON, and interestingly, this boundary spread eastward with time in a similar manner as events studied by Zou et al. [2018]. The flow western boundary was located around -77° MLON during 2120-2134 UT, and started to spread eastward after 2134 UT. Hence the reconnection-related ionospheric flow, once formed, has spread in width and displaced eastward. The spreading has also been noticed in the other two events (see Section 3.3), indicating that this could be a common development feature of the reconnection-related flows. The spreading was fast in the first 6 min and then slowed down stabilizing at a finite flow extent (until the eastern boundary went outside FOV at 2134 UT).

A consequence of the flow temporal evolution is that THA, which was previously outside the reconnection-related flow, became immersed in the flow from 2130 UT, while THE, which was previously inside the flow, was left outside from 2142 UT (Figure 2e). This implies that at the magnetopause the reconnection has spread azimuthally sweeping across THA, and has slid in the –y direction away from THE. This is in perfect agreement with satellite measurements shown in Figures 2q-z. Figures 2q-z presents subsequent magnetopause crossings made by THA and THE following the crossings in Figures 2g-p. THA detected an Alfvenic reconnection jet and a clear D-shape ion

distribution, and THE detected a jet much slower than the Alfvenic speed and an ion distribution without a clear D-shape. This corroborates the connection between the in-situ reconnection signatures with the fast anti-sunward ionospheric flow, and reveals the dynamic evolution of reconnection in the local time direction.

We quantitatively determine the flow extent in Figure 2f. Figure 2f shows the INV LOS velocity profile at 2125 UT as a function of magnetic longitude and distance from 0° MLON. The 2125 UT is the same time instance as in Figures 2a-c and is the time when the flow extent has slowed down from spreading and stabilized. The profile is taken along 80° MLAT. While this latitude is 2° poleward of the open-closed field line boundary, the shape of the flow did not change much over the 2° displacement and thus still presents the reconnection extent. The flow velocity profile has a skewed Gaussian shape, and we quantify the flow azimuthal extent as the full-width-at-half-maximum (FWHM). The FWHM was 13° in MLON or 260 km at an altitude of 260 km. Also shown is the SECS velocity profile. Here we only show the northward component of the SECS velocity as this component represents reconnecting flows across an azimuthally-aligned open-closed field line boundary. The SECS velocity profile gives a FWHM of 13.5° in MLON or 270 km, very similar to the LOS profile.

It is noteworthy mentioning that the velocity profile obtained above approximates to the profile of reconnection electric field along the open-closed field line boundary (details in Figure S3). Reconnection electric field can be estimated by measuring the flow across the open-closed field line boundary in the reference frame of the boundary [Pinnock et al., 2003; Freeman et al., 2007; Chisham et al., 2008]. However, a precise determination of the boundary motion is subject to radar spatial and temporal resolution and for a slow motion like events studied in this paper (Figure S1), the signal to noise ratio is lower than one. For this reason this paper focuses on the velocity profile poleward of the open-closed field line boundary, which is less affected by the error associated with the boundary.

To infer the reconnection extent at the magnetopause, we project the flow width in the

ionosphere to the equatorial plane. The result suggests that the reconnection local time extent was ∼3 Re.

Before closing this section, we would like to point out that the determined extent is characterized by the FWHM of the fast anti-sunward ionospheric flow, which allows weak flows to extend beyond the flow extent. When THA and THE were positioned within the weak flows in the ionosphere, they at the magnetopause observed flows much weaker than the Walen prediction. This may imply that there were two components of reconnection at different scales in this event: weak background reconnection signified by the slow flows, and embedded strong reconnection bursts signified by the fast flows.

Reviewer comment: Line 338: One of the open questions in magnetic reconnection is still how the reconnection rate develops along the length of the X-lines. Since decades of research showed that pulsed reconnection is a rather significant process, it is conceivable that individual sections along a "long" X-line pulse at different frequencies. I therefore would expect that it is very likely that magnetopause crossings by multiple satellites show active and temporarily inactive sections along an X-line. This is not prove that a dayside X-line is short. The interpretation of the authors that this event is a spatially restricted X-line based on flow channels at very different latitudes is not convincing, especially since the satellite observations are outside the flow channels for which observations exist. I also want to stress that in the pulsed reconnection model, field lines that were opened before reconnection briefly stopped, are convecting and provide a continuous transfer of magnetosheath plasma into the magnetosphere. That should certainly influence your radar observations. It is unlikely that the ionosphere would respond that quickly to short changes in the reconnection rate. The magnetosphere is generally rather slow in its response to outside changes. That will make linking ionospheric flow channels to magnetopause observations rather challenging. Radar observations of ionospheric convection, direction and velocities, are often used to estimate global convection pattern in the polar ionosphere using various models. These "convection cells" could be overlayed in the radar plots to make a connection

between the satellite magnetic foot points outside the radar FOV and the radar data. Depending on how these global convection cells look like they might provide a more convincing picture that these observations are actually linked.

Response: We have replaced Figures 1-2 to the new event where the satellite footprints were within the radar FOV and close to the open-closed field line boundary. We believe that this event provides a more convincing case for establishing the space and ground connection.

We agree with the reviewer that reconnection can happen over various temporal scales but the typical time scale of reconnection bursts, or FTEs is found to be a few minutes [Lockwood and Wild, 1993; Kuo et al., 1995; Fasel, 1995]. This can be resolved by radars considering that M-I coupling time scale on the dayside is ∼1-2 min [e.g. Carlson et al., 2004]. Studies have compared the time scale of ionospheric flows with FTEs and found a very similar distribution [McWilliams et al., 1999], suggesting that ionospheric flows well capture reconnection variability at least down to FTE time scale. We add the following text to the end of the methodology section.

"Note that reconnection can happen over various spatial and temporal scales and our space-ground approach can resolve reconnection bursts that are larger than 0.5 Re and persist longer than a few minutes. This is limited by the radar spatial and temporal resolution, and the magnetosphere-ionosphere coupling time which is usually 1-2 min [e.g. Carlson et al., 2004]. This constraint is not expected to impair the result because reconnection bursts above this scale have been found to occur commonly in statistics (see the Introduction section for spatial and Lockwood and Wild [1993], Kuo et al. [1995], Fasel [1995], and McWilliams et al. [1999] for temporal characteristics)."

We have followed the reviewer's opinions and added the global convection pattern in supporting Figure S2. The radars employed in the paper has contributed to the majority of the backscatter on the dayside and including more radars do not change the conclusion. Again we focus on the extent of individual reconnection-related flow,

not the sum of all the flows on the dayside. It may also noteworthy to point out an important difference between our study and previous studies: our events occurred under non-storm time, where the open-closed field line is confined within the utilized few radar FOVs, while previous studies using a wider network of SuperDARN radars focus on storm time period where the boundary has expanded to low latitude.

Interactive comment on Ann. Geophys. Discuss., https://doi.org/10.5194/angeo-2018-63, 2018.

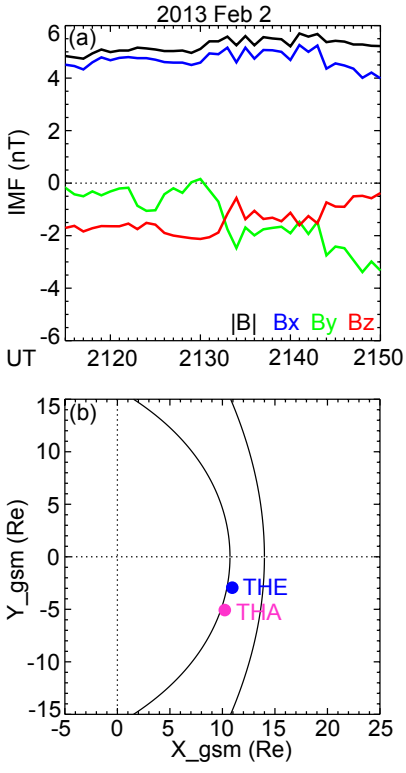

Fig. 1. Figure 1a: OMNI IMF condition on Feb 2, 2013. Figure 1b: THE and THA locations projected to the GSM X-Y plane. The inner curve marks the magnetopause and the outer curve marks the bow shock.

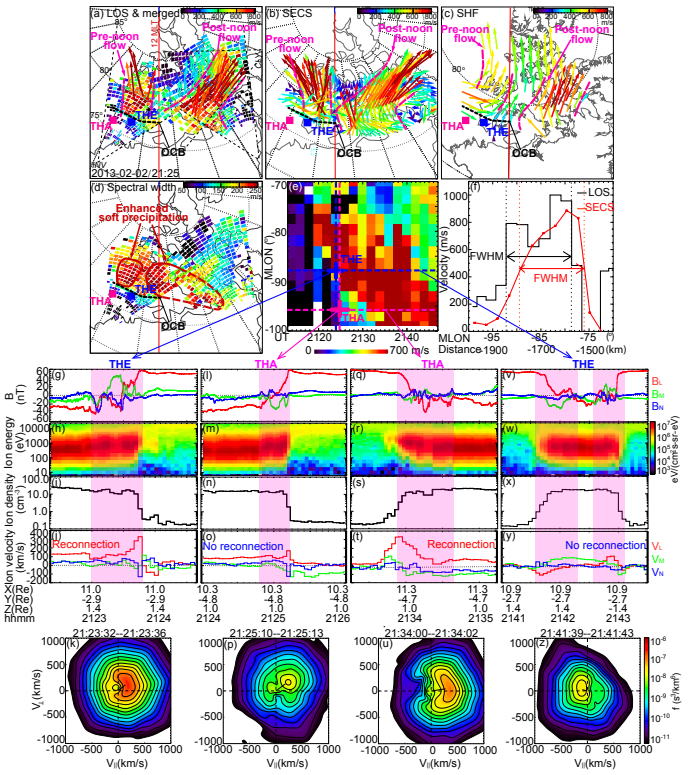

Fig. 2. Figure 2a: SuperDARN LOS speeds (color tiles) and merged velocity vectors (color arrows) in the Altitude adjusted corrected geomagnetic (AACGM) coordinates. The FOVs of the RKN, INV, and CLY radars ar

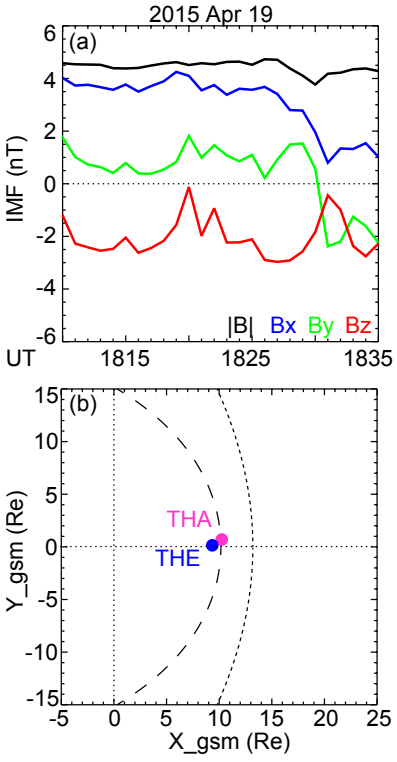

Fig. 3. Figure 3. OMNI IMF condition and THEMIS satellite locations on Apr 19, 2015 in a similar format to Figure 1.

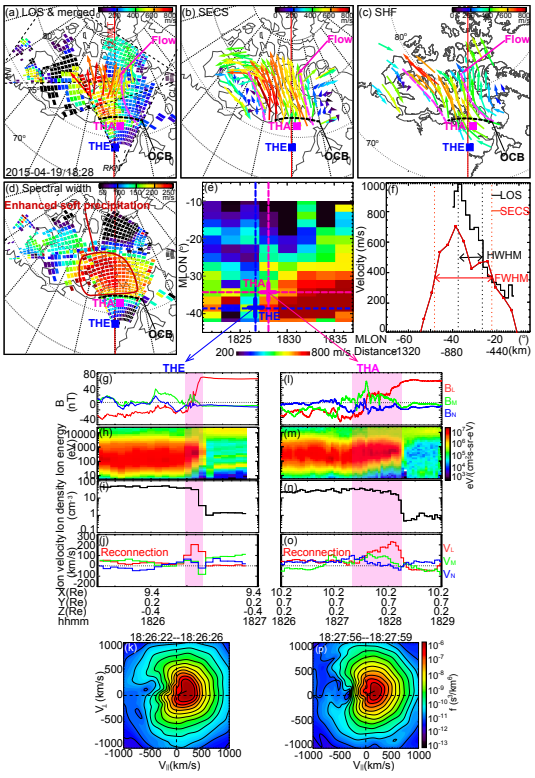

Fig. 4. Figure 4. THEMIS and SuperDARN measurements of reconnection bursts on Apr 19, 2015 in a similar format to Figure 2. The velocity time evolution in Figure 4e and the velocity profile in Figure 4f are t

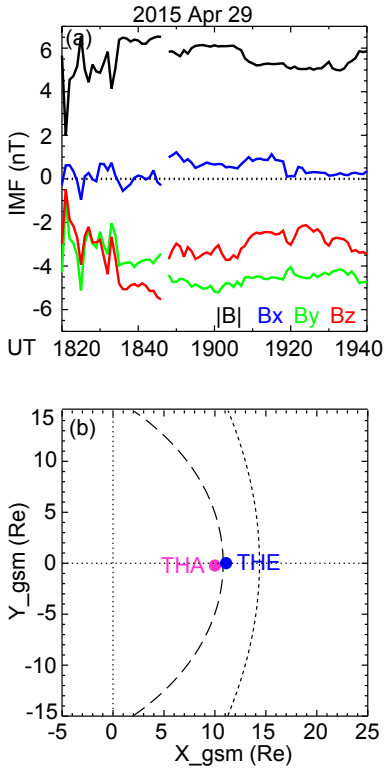

Fig. 5. Figure 5. OMNI IMF condition and THEMIS satellite locations on Apr 29, 2015 in a similar format to Figure 1.

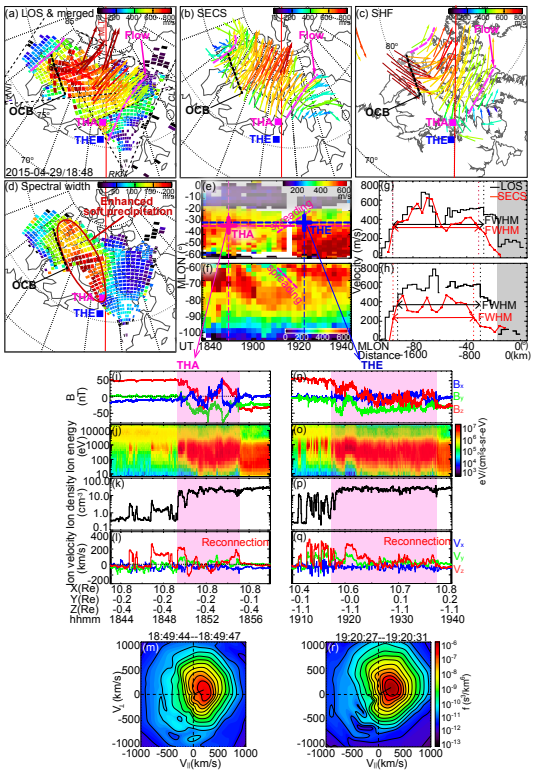

Fig. 6. Figures 6a-d: SuperDARN measurements of reconnection bursts on Apr 29, 2015 in a similar format to Figures 2a-d except that in Figure 6a the color of the CLY color tiles represent LOS speeds towards t

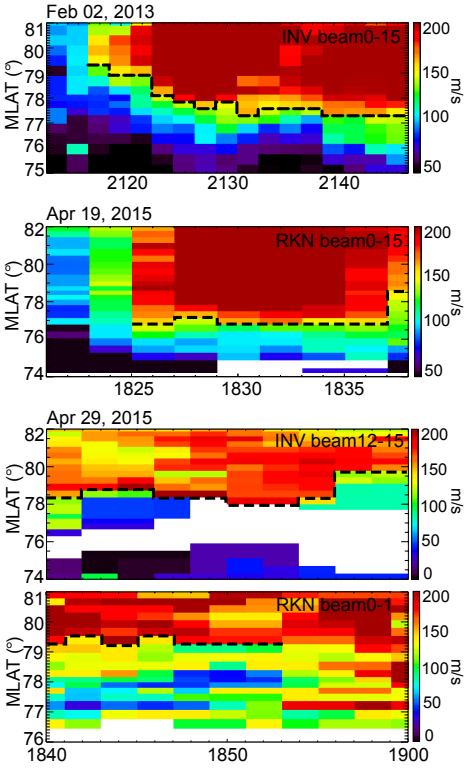

Fig. 7. Figure S1. Location of the open-closed field line boundary (marked by the black dashed line) in the three studied events. The open-closed field line boundary is determined based on the spectral width

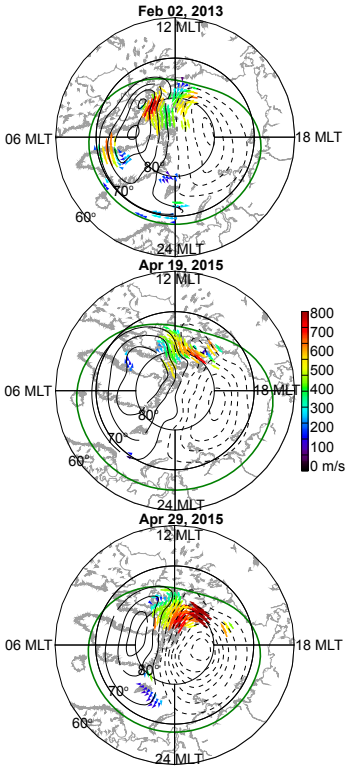

Fig. 8. Figure S2. Global convection maps of the three studied events. The SHF velocities are shown as color arrows, and the contours of the electric potential are shown as black solid (at the duskside) and d

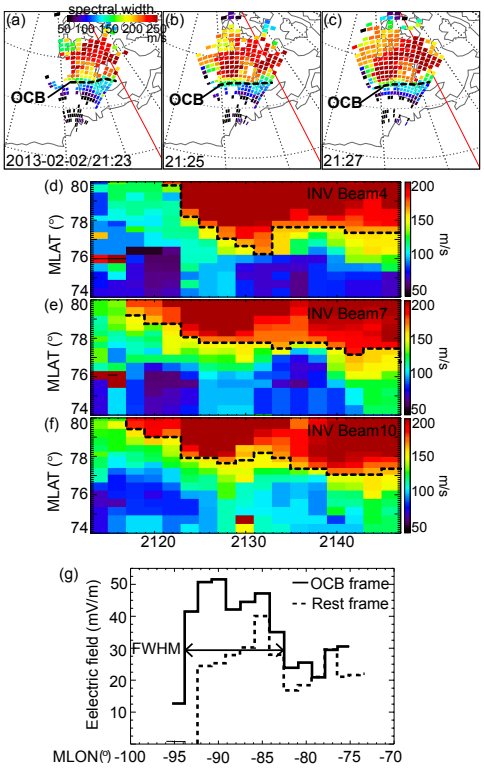

Fig. 9. Figure S3. Reconnection electric along the open-closed field line boundary for the Feb 02, 2013 event. Figures S3a-c: snapshots of spectral width measurements around the space-ground conjunction time